Jurnal Tribologi 19 (2018) 57-78

Jurnal Tribologi
Website : jurnaltribologi.mytribos.org
e-issn: 2289-7232

Parametric investigations of short length hydro-dynamically lubricated conical journal bearing

Ajay K. Gangrade *, Vikas M. Phalle, S. S. Mantha

Machine Dynamics & Vibration Laboratory, Department of Mechanical Engineering,
Veermata Jijabai Technological Institute (VJTI), Mumbai, 400019 INDIA.
*Corresponding author: akgangrade@somaiya.edu

KEYWORD

Conical journal bearing
Hydrodynamic lubrication
Aspect ratio
Eccentricity ratio
Finite element analysis

ABSTRACT

Due to the growing need for compact size fluid film bearings, efforts are being made to explore the performance of hydro-dynamically lubricated short length conical journal bearing. The combined radial and axial load carrying features of these bearings emerge as a better option to replace the two separate bearings (journal and thrust pad bearings) employed in turbo-machines and other applications. Thus, in this study, attempts have been made to investigate the performance of conical hydrodynamic journal bearing by using finite element analysis. The bearings have been investigated for semi-cone angle (γ = 10°), aspect ratio (λ = 0.5, 0.8, 1.0), journal speed (v = 2.6, 5.2 m/s) and load variations in terms of eccentricity ratio (ε) up to 0.6. Results have been presented in terms of radial and axial load carrying capacity, stiffness coefficients, damping coefficients and threshold speed. Results from the present study reveal that load carrying capacity is improved with higher aspect ratio; whereas threshold speed decreases with the increase of eccentricity ratio and aspect ratio.

Received 24 April 2018; received in revised form 16 August 2018; accepted 7 Sept 2018.
To cite this article: Gangrade et al. (2018). Parametric investigations of short length hydro-dynamically lubricated conical journal bearing. Jurnal Tribologi 16, pp.57-78.

NOMENCLATURE

C_{ij}	damping coefficient, (*i, j*=1,2), Ns/m
C	radial clearance, μm
C/Rj	clearance ratio
d	mean journal diameter, *mm*
e	journal eccentricity, *mm* $(e^2 = x^2 + z^2)$
$e_o ; \varphi_o$	journal eccentricity and attitude angle at initial equilibrium position
F	fluid film reaction $\frac{\partial h}{\partial t} \neq 0$, *N*
F_o	fluid film reaction $\frac{\partial h}{\partial t} = 0$, *N*
$F_x; F_z$	fluid film reaction component in X and Z direction, $\frac{\partial h}{\partial t} \neq 0$, *N*
$F_a; F_r$	fluid film reaction component in axial and radial direction, $\frac{\partial h}{\partial t} \neq 0$, *N*
h	fluid film thickness, *mm*
h_{min}	minimum fluid film thickness, *mm*
L	bearing length, *mm*
o_1, o_2	bearing and journal center
N_i, N_j	shape functions
p	fluid film pressure, *MPa*
p_{max}	maximum fluid film pressure, *MPa*
p_s	supply pressure, *MPa*
R_b	mean bearing radius, *mm*
R_j	mean journal radius, *mm*
R_1	minimum journal radius, *mm*
R_2	maximum journal radius, *mm*
S_{ij}	fluid film stiffness coefficients (*i, j* =1, 2), *N/m*
t	time, *sec*
W	external load, *N*
W_a	axial load, *N*
W_r	radial load, *N*
X,Y,Z	cartesian coordinates, *mm*
x, z	horizontal, vertical journal eccentricity , *mm*
X_j, Z_j ; $\dot{X}_j, \dot{Z}_j$	journal center displacement and velocity components , *mm; mm/s*
$\bar{X}_J, \bar{Z}_J$	initial steady state position with zero initial velocity ($\dot{\bar{X}}_J = 0$; $\dot{\bar{Z}}_J = 0$)

Greek symbols

α	circumferential coordinate (ϕ)
β	axial coordinate ($r \sin \gamma / R_j$)
γ	semi-cone angles
ε	journal eccentricity ratio (e/c)

r, ϕ, γ	spherical coordinates for conical bearing, radial distance; *mm,* azimuthal angle*; radian* and polar angle*; radian*
φ	attitude angle, *rad*
λ	aspect ratio (L/d)
ρ	mass density of lubricating fluid, *kg/ m³*
μ	lubricant fluid absolute or dynamic viscosity, *Ns/m²*
μ_r	dynamic viscosity at reference inlet temperature and atmospheric pressure, *Ns/m²*
v	Journal relative velocity, *m/s*
ω	journal angular velocity, *rad/s*
Ω	threshold speed parameter, $\omega(\mu R_j^2/C^2\, p_s)$

Other symbols

$\bar{C}_{ij}$	damping coefficient
$\bar{C}_{11}, \bar{C}_{22}$	direct damping coefficients
$\bar{h}$	fluid film thickness, (h/c_r)
$\bar{h}_{min}$	minimum fluid film thickness, (h_{min}/c_r)
$\bar{M}_{cr}$	critical mass parameter, $M_{cr}(c_r{}^5 p_s/\mu^2 R_j^6)$
N_j	shape function
ξ, η	local coordinates system for shape function N_j
$\bar{p}$	pressure ratio, (p/p_s)
$\bar{p}_j$	pressure ratio at jth nodal point, (p_j/p_s)
$[\bar{F}]$	assembled fluidity matrix
$\{\bar{p}\}$	nodal pressure vector
$\{\bar{Q}\}$	nodal flow vector
$\{\bar{R}_H\}$	column vector due to hydrodynamic terms
$\{\bar{R}_{x_j}\}, \{\bar{R}_{z_j}\}$	global vectors due to journal center linear velocities
$\bar{S}_{ij}$	dimensionless stiffness coefficient
$\bar{S}_{11}, \bar{S}_{22}$	dimensionless direct stiffness coefficients
$\bar{W}_a$	axial load, ($\bar{W}_a = \frac{W_a}{p_s R_j^2}$)
$\bar{W}_r$	radial load, ($\bar{W}_r = \frac{W_r}{p_s R_j^2}$)
$\bar{\mu}$	dynamic viscosity, (μ/μ_r)
$\bar{\omega}_{th}$	threshold speed margin
$\bar{t}$	Time, t $(C^2 p_s/\mu R_j^2)$
$\Delta\bar{X}_J, \Delta\bar{Z}_J$	small amount of journal movement from steady state equilibrium journal center
$\bar{X}_J = X_J/C,$ $\bar{Z}_J = Z_J/C$	dimensionless coordinates of steady state equilibrium journal center
$\Delta\dot{\bar{X}}_J, \Delta\dot{\bar{Z}}_J$	dimensionless velocity components of journal center

1.0 INTRODUCTION

Conical hydrodynamic journal bearing has an ability to support the radial and axial loads together. Thus, exploration of performance behavior of conical bearing for its proper development to replace the two separate bearings (journal bearing and thrust pad bearing) with a single compact bearing is a vital and interesting task. It is worth mentioning here that the hydrodynamic conical journal bearings involve low cost, ease of manufacture and compact size as compared to two separate bearings presently employed in turbo-machines and other applications (Kim et al., 2017). The stability behavior of the hydrodynamic journal bearing is one of the core concerns at the design stage and is essential to ensure the proper operation of the rotor-bearing system. Thus, a study has been carried out to explore the performance of compact size conical hydrodynamic journal bearing for a wide range of operating parameters.

In the past, attempts have been made by many researchers to study the performance of conical journal bearing under different operating conditions with certain assumptions and considerations. Six-lobed (in form of scallops) conical bearing was theoretically analyzed by Murthy (1981) and he revealed that the performance behavior of a bearing is a very strong function of lobe's depth and radial clearance. Yousif and Nancy (1994) used numerical and experimental methods to investigate the performance of conical bearing and reported that the presence of solid additives in lubricating oil enhances the load carrying capacity of bearing. Korneev (2012) studied the performance characteristics of plain/multiple wedge hydrodynamic and hybrid conical journal bearing with turbine oil as a lubricant and presented the formulae for the load-carrying capacity. He has reported that the performance is improved with the increase in speed and radial eccentricity. The fluid flow in the immobile conic surfaces was studied by Gamal and Al-Hanaya (2014) and they have presented the numerical results in the form of non-dimensional charts for radial and axial load carrying capacity. Moreover, the pressure distribution and load carrying capacity were also explored by other research scholars Czaban (2013) in their respective studies of hydro-dynamically lubricated conical journal bearings. However, Chen et al. (2015) have used gas for lubrication in the conical journal bearing in place of conventional oil lubricant and investigated the basic tribological performance parameters.

Stability performance behavior of hydro-dynamically lubricated conical journal bearings were investigated by Hong et al. (2009) and they have characterized the fluid film force in terms of linear stiffness and damping coefficients in order to discuss the stability concerns. In their analytical and experimental work, they have observed that hybrid conical journal bearing has the advantages of high load carrying capability and high stability for small eccentricity ratio. Garg (2015) computed and presented the results for Newtonian and Non-Newtonian lubricants in terms of stiffness coefficients, damping coefficients, and threshold speed for fluid film hybrid journal bearing. Recently Ram (2016a; 2016b) studied modified Reynolds equation for a non-recessed fluid film hybrid journal bearing system and solved using finite element method. He reported that under varying Reynolds number, the rotor dynamic coefficients of bearing are found higher than the laminar regime. Authors (Korneev and Yaroslavtsev, 2010) proposed the formulae for evaluation of stiffness and damping coefficients for oil lubricated grooved conical journal bearing (which researchers have named multi-pad bearing). However, some researchers (Kim et al., 2012) have derived a generalized Reynolds equation and its perturbation equations to calculate the characteristics of a conical bearing. The dynamic characteristics of conical journal bearing have been presented for the variation in the fluid film thickness and semi-conical angles. In all such investigations, mainly variations of bearing coefficients (stiffness and damping) have been studied and presented by the authors.

Application of double conical journal bearings in a high-speed centrifugal pump is studied by Ettles and Svoboda (1975). They have reported the limitations of a double inclined journal bearing and in another study, they have discussed the effect of aspect ratio on the stability of circular bearing. Effect of aspect ratio on the performance of fluid film bearing system is presented by Sharma and Awasthi (2016) using numerical methods. In another study, Sharma and Awasthi (2017) presented the effect of aspect ratio on the stability performance parameters of the worn hydrodynamic journal bearing. Other authors (Sharma and Krishna, 2015) also studied the effect of aspect ratio on the dynamic performance of two-lobe pressure dam bearing and their results show that stability of two-lobe pressure dam bearings increases with a decrease in aspect ratio. It was seen in one of the studies reported by Yadav and Ram (2018) that two-lobe journal bearing is more stable as compared to circular journal bearing. Rana et al. (2016) presented the performance characteristics of a four-pocket conical hydrostatic journal bearing for various values of semi-cone angle and aspect ratio. Bearing size in terms of aspect ratio is always an important study in the fluid film bearing for research scholars.

Based on the literature review, it is observed that there is no measurable study on performance analysis of hydro-dynamically lubricated conical journal bearing. It is also revealed that the effect of aspect ratio on the stability behavior of conical journal bearings is not yet fully publicized. Thus, in the present work, attempts have been made to investigate the performance behavior of hydro-dynamically lubricated short length conical journal bearing by using Finite Element Analysis. The bearing performance has been investigated for semi-cone angle (γ = 10°), aspect ratio (λ = 0.5, 0.8, 1.0), journal speed (v = 2.6, 5.2 m/s) and load variations in terms of eccentricity ratio (ε) up to 0.6. Results have been presented in terms of radial and axial load carrying capacity, stiffness coefficients, damping coefficients and threshold speed. The main objective of this paper is to provide an insight for selection of compact size conical journal bearing for combined radial and the constant axial load acting on rotating journal.

2.0 GOVERNING EQUATIONS AND FINITE ELEMENT FORMULATIONS

Reynolds equation is used for the formulation of a conical hydrodynamic journal bearing problem in this section. The schematic view of a conical hydrodynamic journal bearing supported by a fluid film in clearance space is shown in Fig. (1). Also, the expressions for static and dynamic characteristics are presented in this section for hydrodynamic journal bearing.

2.1.1 Reynolds equation

Reynolds equation is used for computation of fluid film pressure under steady state equilibrium condition of the journal in the clearance space of bearing. The time-dependent equation governing the fluid flow in the clearance space of bearing is expressed as follows Sharma et al. (2011a; 2011b):

$$\frac{1}{r}\frac{\partial}{\partial r}\left(\frac{r}{12\mu}h^3\frac{\partial p}{\partial r}\right)+\frac{1}{sin^2\gamma}\frac{\partial}{\partial \phi}\left(\frac{h^3}{12\mu}\frac{1}{r^2}\frac{\partial p}{\partial \phi}\right)=\frac{\omega}{2}\frac{\partial h}{\partial \phi}+\frac{\partial h}{\partial t} \quad (1)$$

Where; r, γ, ω, μ, p and h, represent the journal radius, semi-cone angle, journal rotational speed, viscosity of the lubricating fluid, fluid pressure and fluid film thickness respectively.

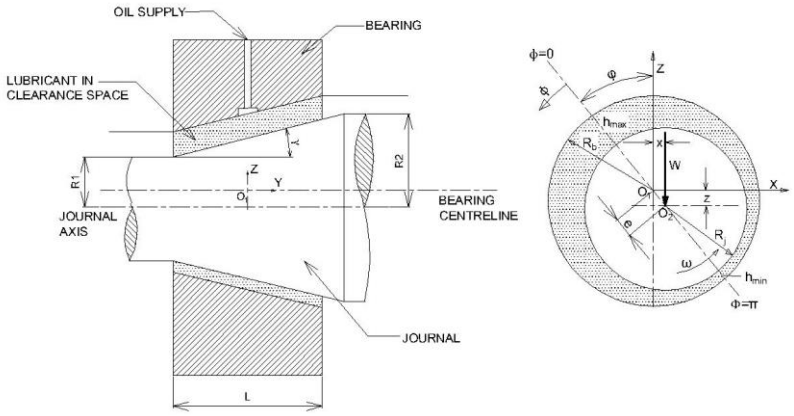

(a)

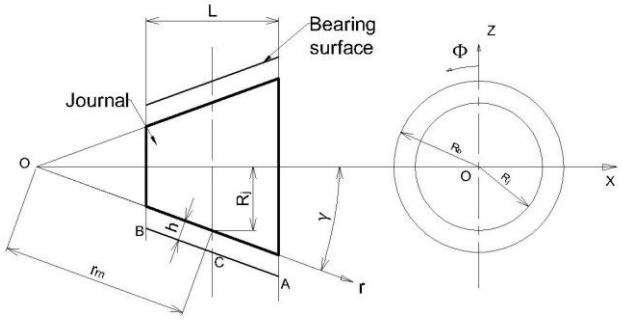

(b)

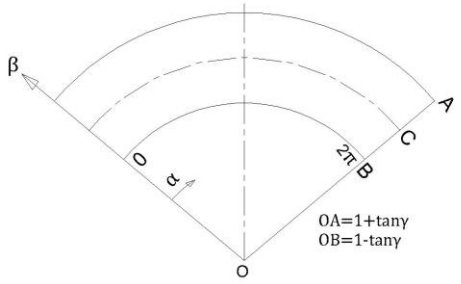

$$\alpha = \phi; \qquad \beta = {r \sin \gamma}/{R_j}$$

(c)

Figure 1: Schematic view of a conical hydrodynamic journal bearing with spherical coordinate system (a) Conical hydrodynamic journal bearing in eccentric position (b) Spherical coordinate system (r, ϕ, γ) and (c) Developed conical bearing surface.

The Eqn. (1) is derived in the spherical coordinate system (r, ϕ, γ) as (radial distance, azimuthal angle, polar angle) for conical hydrodynamic journal bearing. Whereas, spherical coordinates in non-dimensional form are specified as (β = r, $\alpha = \phi$, *and* $\gamma = \gamma$*)* in Reynolds equation and expressed as Eqn. (2). The similar governing equation is used in a spherical coordinate system

with non-zero values of γ by (Gamal, 2004; Bassani and Piccigallo, 1992; and Sharma et al. (2011a; 2011b) in their research work.

$$\frac{\partial}{\partial\beta}\left((sin^2\gamma)\beta\frac{\bar{h}^3}{12\bar{\mu}}\frac{\partial\bar{p}}{\partial\beta}\right)+\frac{\partial}{\partial\alpha}\left(\frac{1}{\beta}\frac{\bar{h}^3}{12\bar{\mu}}\frac{\partial\bar{p}}{\partial\alpha}\right)=\frac{\Omega}{2}\frac{\partial\bar{h}}{\partial\alpha}+\frac{\partial\bar{h}}{\partial\bar{t}} \quad (2)$$

Where; $\alpha=\phi$; β = axial coordinate of the cone and is represented as; $\beta = {}^{r\,sin\,\gamma}/_{R_j}$

$\bar{p} = {}^{p}/_{p_s}$; $\bar{\mu} = {}^{\mu}/_{\mu_r}$; $\bar{h} = {}^{h}/_{C}$; $\bar{t} = {}^{t}/_{\mu R_j^2/C^2 p_s}$; $\Omega = \omega_J\left(\mu R_j^2/C^2\,p_s\right)$;

In hydrodynamic journal bearing, fluid film thickness (h) is very small as compared to the bearing length (L) and mean radius of journal (R_j), i.e. (h/L) ; (h/R_j) <<< 1, hence, the effect of film curvature on bearing performance has been neglected and the rotational velocity of journal can be changed with the linear velocity. The boundary conditions used for the analysis of lubricant flow field are described as follows (San Andres, 1991).

i. The pressure is periodic in the circumferential direction-

$$\bar{p}\,(\alpha,\beta,t) = \bar{p}\,(\alpha+2\pi,\beta,t) \quad (3a)$$

ii. The pressure equals the atmospheric pressure on the bearing sides/edges-

$$\bar{p}\,(\alpha,(\beta=-1),t\,) = \bar{p}\,(\alpha,(\beta=+1),t) = 1 \quad (3b)$$

iii. Reynolds boundary conditions are employed for a solution and assumed that pressure and pressure derivative are equal to zero at the outlet condition ($\alpha=\theta_2$).

$$\bar{p}\ \geq\ \bar{p}_{cav};\ in\ 0\ \leq\ \alpha\leq 2\pi;\ -1\leq\beta\ \leq+1 \quad (3c)$$

$$\bar{p})_{\alpha=0} = 0;\ \bar{p})_{\alpha=\theta_2} = 0;\ \ \frac{\partial\bar{p}}{\partial\alpha})_{\alpha=\theta_2} = 0 \quad (3d)$$

2.1.2 Finite element formulation

In Finite element formulation, for simplicity of the solution, the computational domain has been discretized by using four noded isoparametric elements. Each element is represented by the corresponding corner node number and the element is identified by the number at the center of the element. Figure 2 illustrates the discretized computational domain of bearing surface with 48 elements and 60 nodes.

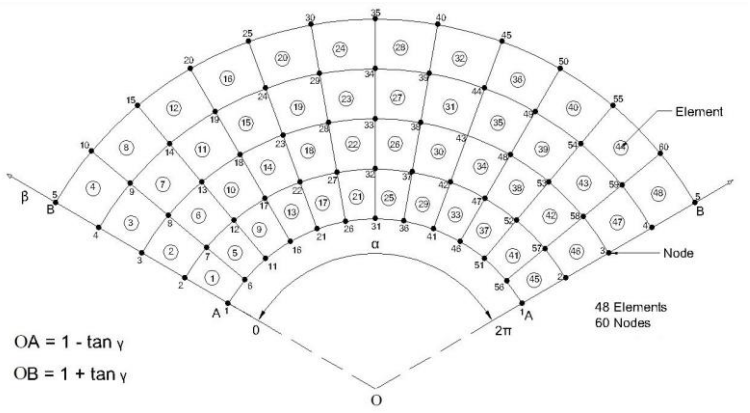

Figure 2: Discretized view of the computational domain.

Following Lagrangian interpolation function, used for pressure calculation at nodal points, incorporating the boundary conditions:

$$\bar{p} = \sum_{j=1}^{4} N_j \, \bar{p}_j \tag{4a}$$

Where N_j is the shape function for the linearly interpolated isoparametric element. Shape function N_j is expressed in terms of local coordinates (ξ, η) as follows:

$$\begin{aligned} N_1 &= \frac{1}{4}(1-\xi)(1-\eta) \\ N_2 &= \frac{1}{4}(1+\xi)(1-\eta) \\ N_3 &= \frac{1}{4}(1+\xi)(1+\eta) \\ N_4 &= \frac{1}{4}(1-\xi)(1+\eta) \end{aligned} \tag{4b}$$

$$\bar{p}^e = \left[N_1, N_2, N_3, N_4\right] \begin{Bmatrix} \bar{p}_1 \\ \bar{p}_2 \\ \bar{p}_3 \\ \bar{p}_4 \end{Bmatrix} \tag{4c}$$

Galerkin's technique is used to minimize the residue by orthogonality condition using the value of $\bar{p}$ in Eq. (2), and then the typical element equation in matrix form is as follows Sharma et al. (2011a; 2011b):

$$[\bar{F}]^e\{\bar{P}\}^e = [\bar{Q}]^e + \Omega\{\bar{R}_H\}^e + \dot{\bar{x}}_j \left\{\bar{R}_{x_j}\right\}^e + \dot{\bar{z}}_j \left\{\bar{R}_{z_j}\right\}^e \tag{5}$$

The resulting equation for all the elements is obtained and assembled in global matrix form, which can be expressed as follows.

$$[\bar{F}]\{\bar{P}\} = [\bar{Q}] + \Omega\{\bar{R}_H\} + \dot{\bar{x}}_j\left\{\bar{R}_{x_j}\right\} + \dot{\bar{z}}_j\left\{\bar{R}_{z_j}\right\} \quad (6)$$

Where;
$[\bar{F}]$ = assembled fluidity matrix,
$\{\bar{P}\}$ = nodal pressure vector,
$[\bar{Q}]$ = nodal flow vector,
$\{\bar{R}_H\}$ = column vectors due to hydrodynamic terms,
$\left\{\bar{R}_{x_j}\right\}, \left\{\bar{R}_{z_j}\right\}$ = global right-hand side vectors due to journal center linear velocities.

The total pressure at a node point (jth node) in the flow field is given by the expression:

$$\bar{P}_j = \bar{P}_j\,(\bar{X}_j, \bar{Z}_j, \dot{\bar{X}}_j, \dot{\bar{Z}}_j) \quad (7)$$

Where the pressure is the function of journal steady-state position $(\bar{X}_J, \bar{Z}_J)$ and; if initial steady state position with zero initial velocity $(\dot{\bar{X}}_J = 0;\ \dot{\bar{Z}}_J = 0)$ is assumed, then initial flow field condition is as follows:

$$\bar{P}_j = \bar{P}_j\left(\bar{X}_J, \bar{Z}_J\right) = \bar{P}_o \quad (8)$$

Where, $\bar{P}_o$= steady state nodal pressure. After modifications, for necessary boundary conditions, the Eq. (6) is solved for nodal pressure using a linearized perturbation method applied to Reynolds equation.

2.1.3 Fluid film thickness

The bearing surface in a full lubricated region kept apart with the nominal fluid film thickness (h) so as to avoid the metal-to-metal contact. The fluid film thickness of the conical journal bearing system is generally represented in nondimensional form as Sharma et al. (2011a; 2011b)

$$\bar{h} = \left(1 - \bar{X}_j\ cos\,\alpha - \bar{Z}_j\ sin\,\alpha\right) cos\,\gamma \quad (9)$$

Above equation is written assuming bearing and journal surfaces as rigid and uniform axial and azimuthal clearances with no journal misalignment in the bearing.

2.1.4 Load carrying capacity

The hydrodynamic forces developed on the bearing surface by the fluid film can be evaluated by integrating the fluid pressure over the contact surface area of bearing.

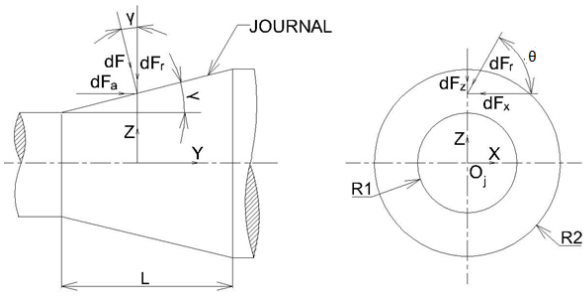

Figure 3: Load carrying capacity distribution of a conical journal bearing.

The components of forces in radial and the axial direction ($\bar{F}_r, \bar{F}_a$) are shown in Fig. 3 and expressed in Eqs.10 (a) and 10(b). Whereas, the resultant radial force ($\bar{F}_r$) acts on journal center at an angle θ in x-z plane and further resolved into *X* and *Z* directions ($\bar{F}_x$ and $\bar{F}_z$) as stated in Eqs. 10(c) and 10(d), as follows (Rajput, 2013).

$$\bar{F}_r = \bar{F} cos\gamma = -\int_{-\lambda}^{\lambda}\int_{0}^{2\pi} \bar{p}\, cos\gamma \; d\alpha \; d\beta \tag{10a}$$

$$\bar{F}_a = \bar{F} sin\gamma = -\int_{-\lambda}^{\lambda}\int_{0}^{2\pi} \bar{p}\, sin\gamma \; d\alpha \; d\beta \tag{10b}$$

$$\bar{F}_x = \bar{F}_r cos\theta = -\int_{-\lambda}^{\lambda}\int_{0}^{2\pi} \bar{p}\, cos\theta \; cos\gamma \; d\alpha \; d\beta \tag{10c}$$

$$\bar{F}_z = \bar{F}_r \; sin\theta = -\int_{-\lambda}^{\lambda}\int_{0}^{2\pi} \bar{p}\, sin\theta \; cos\gamma \; d\alpha \; d\beta \tag{10d}$$

2.1.5 Fluid film dynamic coefficients

The fluid-film stiffness ($\bar{S}_{ij}$) and damping coefficients ($\bar{C}_{ij}$) have been evaluated as a function of the relative displacement and velocity of the journal center with respect to bearing center. If the dynamic pressure fields are known, then all non-dimensional stiffness and damping coefficients can be easily acquired for the performance analysis.

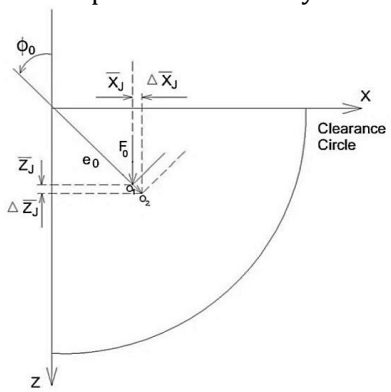

Figure 4: Schematic representations of journal perturbation of lubricating film in bearing.

Fluid film reaction components on the journal are calculated by integration of pressure field acting on the journal surface. Figure 4 shows the small magnitude of journal displacement $\left(\Delta\bar{X}_J, \Delta\bar{Z}_J\right)$ about the initial journal position and fluid film replaced by symbolic dynamic coefficients for journal bearing. In stability analysis of conventional fluid film hydrodynamic journal bearing Lund J.W. (1974), suggested that performance of bearing is mainly dependent on radial components of fluid film stiffness and damping coefficients i.e. direct dynamic coefficients $K_{xx}, K_{yy}, C_{xx}, C_{yy}$ and cross coupled coefficients $K_{xy}, K_{yx}, C_{xy}, C_{yx}$. The fluid film stiffness coefficients are expressed as follows:

$$\bar{S}_{ij} = -\frac{\partial \bar{F}_i}{\partial \bar{q}_j} \; ; \; (i, j = X, Z) \tag{11}$$

Where; 'i' is the direction of force,
'$\bar{q}_j$' is the direction of journal center displacement i. e. $\left(\bar{q}_j = \bar{X}_J, \bar{Z}_J\right)$

For the computation of stiffness coefficients($\bar{S}_{ij}$), the nodal pressure derivatives under steady-state conditions are calculated with respect to new journal location ($\bar{X}_J, \bar{Z}_J$). Whereas, the damping coefficients ($\bar{C}_{ij}$) are evaluated with respect to journal center velocities as follows:

$$\bar{C}_{ij} = -\frac{\partial \bar{F}_i}{\partial \dot{\bar{q}}_j} \; ; \; (i, j = X, Z) \tag{12}$$

Where; '$\dot{\bar{q}}_j$' represent the velocity component of the journal center for calculation of damping coefficients ($\bar{C}_{ij}$), the nodal pressure derivatives under steady-state conditions are to be calculated with respect to new journal location ($\bar{X}_J, \bar{Z}_J$).

2.1.6 Stability parameters for a linearized system

In the present work, the stability limit of the rotor speed is obtained for a system consisting of a single rotor disc in the middle of a flexible shaft having identical bearings at the ends as discussed by Rahmani et al. (2016a; 2016b), Bhattacharya et al. (2017) and Javorovo et al. (2009). The stability parameter in terms of threshold speed ($\bar{\omega}_{th}$) of the journal bearing is obtained using the Routh's stability criteria. The non-dimensional threshold speed ($\bar{\omega}_{th}$) is obtained by using the relation given below (Khakse et al., 2016).

$$\bar{\omega}_{th} = \left[\bar{M}_{cr} \Big/ \bar{F}_0\right]^{1/2} \tag{13}$$

Where, $\bar{\mathrm{F}}_0$ is the resultant fluid-film force at $\frac{\partial \bar{\mathrm{h}}}{\partial \bar{\mathrm{t}}} = 0$. $\overline{M}_{cr}$, is a dimensionless critical mass for lateral movement of the journal and evaluated by using the stiffness and damping coefficients. It is expressed as:

$$\bar{M}_{cr} = \frac{\bar{G}_1}{\bar{G}_2 - \bar{G}_3} \tag{14}$$

Where, $\bar{G}_1 = [\bar{C}_{xx}\bar{C}_{zz} - \bar{C}_{xz}\bar{C}_{zx}]$;

$$\bar{G}_2 = \frac{[\bar{S}_{xx}\bar{S}_{zz} - \bar{S}_{xz}\,\bar{S}_{zx}][\bar{C}_{xx} + \bar{C}_{zz}]}{[\bar{S}_{xx}\bar{C}_{zz} + \bar{S}_{zz}\bar{C}_{xx} - \bar{S}_{xz}\,\bar{C}_{zx} - \bar{S}_{zx}\bar{C}_{xz}]}$$

$$\bar{G}_3 = \frac{[\bar{S}_{xx}\bar{C}_{xx} + \bar{S}_{xz}\,\bar{C}_{xz} + \bar{S}_{zx}\bar{C}_{zx} + \bar{S}_{zz}\bar{C}_{zz}]}{[\bar{C}_{xx} + \bar{C}_{zz}]}$$

A journal bearing is asymptotically stable when the operating speed of the journal is less than the threshold speed i.e. when ($\omega < \Omega$). Threshold speed is the speed at which the bearing remains stable and a further increase in rotational speed will induce whirling at a subsynchronous frequency, that is equal to a natural frequency of the journal-bearing system.

3.0 COMPUTATIONAL PROCEDURE

Finite Element Method is used to solve modified Reynolds equation governing the flow of lubricant in the clearance space of a conical hydrodynamic journal bearing. The initial steady state position ($\bar{X}_J, \bar{Z}_J$) with zero initial velocity ($\dot{\bar{X}}_J = 0$ and $\dot{\bar{Z}}_J = 0$) is assumed for journal center coordinates and then the equation is solved for pressure field. The overall solution of Eq. (6) has been obtained for the specified vertical external load. In the present study, an iterative procedure is continued till the final position of journal center is reached.

The increment in journal center coordinates is used for calculation of the nodal values of fluid film thickness and thereafter the fluidity matrices are generated for each element. The system equation for specified boundary conditions has been solved for the nodal pressure using the Gaussian elimination technique. The solution of system equation has been obtained using Taylor series for i^{th} journal center position to establish the equilibrium journal center position using the following equations:

$$\begin{aligned} \bar{F}_x &= 0 \\ \bar{F}_z &= \bar{W}_r \\ \bar{F}_y &= \bar{W}_a \end{aligned} \tag{15}$$

Correction in the journal center displacements are obtained and the new position of journal center $\left(\bar{X}_J^{i+1},\ \bar{Z}_J^{i+1}\right)$ are represented as:

$$\begin{aligned} \bar{X}_J^{i+1} &= \bar{X}_J^{i} + \Delta\bar{X}_J^{i} \\ \bar{Z}_J^{i+1} &= \bar{Z}_J^{i} + \Delta\bar{Z}_J^{i} \end{aligned} \tag{16}$$

Where, $\bar{X}_J^i$, $\bar{Z}_J^i$ are the coordinate of the journal center position as shown in Fig. 4. The iterative solutions for calculation are continued till the convergence criterion (17) is satisfied. The iterative solution procedure is shown in Fig.5 and the parameters used for the analysis of hydrodynamic conical journal bearing are expressed in Table 1.

$$\left[\frac{\left(\left(\Delta_{\bar{X}_J^i}\right)^2 + \left(\Delta_{\bar{Z}_J^i}\right)^2\right)^{1/2}}{\left((\bar{X}_J^i)^2 + (\bar{Z}_J^i)^2\right)^{1/2}}\right] 100 < 0.001 \tag{17}$$

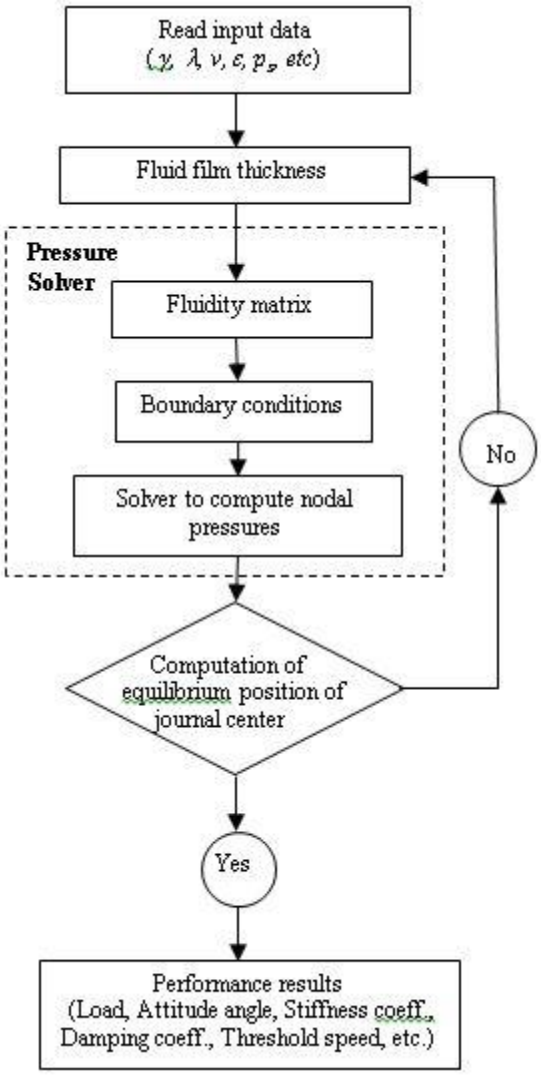

Figure 5: Flowchart for computation of performance results.

Table 1: Operating and Geometric Parameters for conical hydrodynamic journal bearing

Bearing parameters	**Value**	**Bearing parameters**	**Value**
Aspect ratio ($\lambda = L/d$)	0.5, 0.8, 1.0	Mean journal radius (R_j), *mm*	50
Bearing length (L), *mm*	100	Clearance ratio (C/R_j)	0.001
Radial clearance (C), μm	50	Semi cone angle (γ)	10^o
Eccentricity Ratio (ε)	0.1 – 0.6	Supply pressure (p_s), *MPa*	0.5
Relative velocity (v), *m/s*	2.6, 5.2	Lubricant viscosity (μ), *Pa-s*	0.0277

4.0 RESULTS AND DISCUSSION

In the present work, performance characteristics for short length conical hydrodynamic journal bearing have been presented and discussed for various parameters in aligned conditions, i.e. semi-cone angle (γ = 10°), aspect ratio (λ = 0.5, 0.8, 1.0), journal speed (v = 2.6, 5.2 *m/s*) and load variations in terms of eccentricity ratio (ε) up to 0.6. A computer code has been developed in Fortran-77 and used for computing the performance characteristics of the hydrodynamic conical journal bearing. Results have been discussed in this section for load carrying capacity, stiffness coefficients, damping coefficients and stability parameter in terms of threshold speed. Further, the bearing performance has been compared with a corresponding base bearing i.e. conical hydrodynamic journal bearing of semi-cone angle (γ = 10°) and aspect ratio (λ =1.0).

In order to verify the calculated numerical results and confirm the methodology used for this analysis; the numerically simulated results have been validated on customized manufactured conical hydrodynamic journal bearing test rig (CHJB-test-rig) for a semi-cone angle (γ = 10°) and aspect ratio (λ = 1) at the Machine Dynamics and Vibration Laboratory, VJTI, Mumbai India. The CHJB-test-rig devised for this purpose is capable to measure the pressure distribution at selected points in a conical journal bearing, as shown in Fig. 6. In CHJB-test-rig, all physically relevant parameters have been taken into account with the FEA simulation model of the conical journal bearing for semi-cone angle (γ = 10°). On the circumference of conical bearing, at the midplane 8 predefined positions are used for instrumentations as shown in Fig. 6(b). In this study, 5 ports (P_1, P_2, P_3, P_4, and P_5) are used for measuring the pressure, 2 ports (T_1 and T_2) are used for temperature measurement and 1 port (IP_1) is utilized for oil supply to the bearing. The experimental results for pressure at these positions have been compared with the FEA results. Figure 7 shows a good agreement between numerical and experimental results.

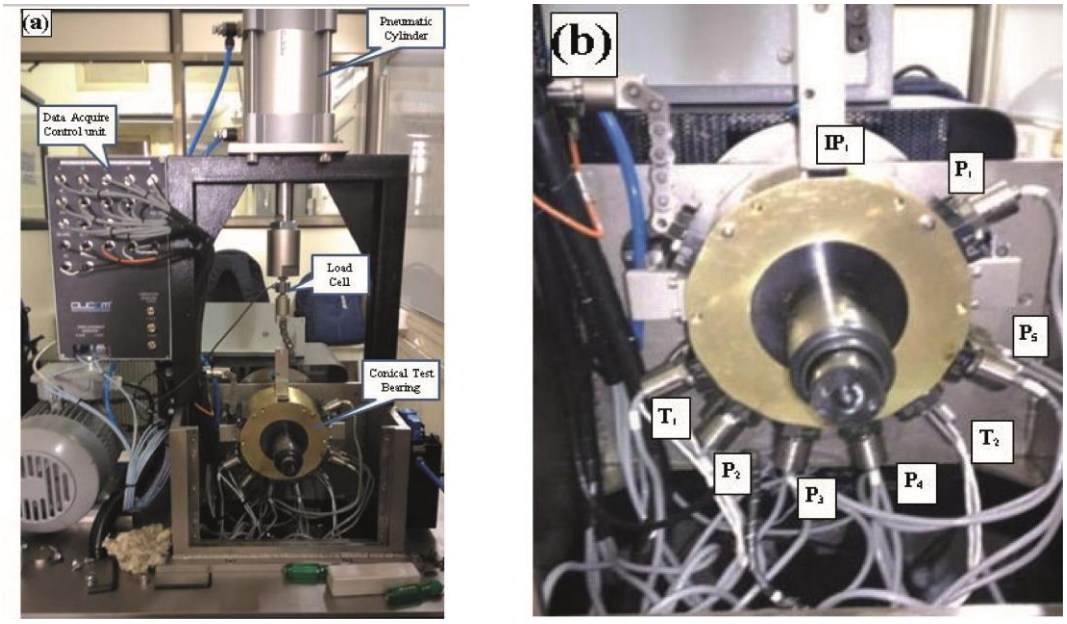

Figure 6: (a) Conical hydrodynamic journal bearing and (b) 8 ports for mounting the pressure and temperature sensors.

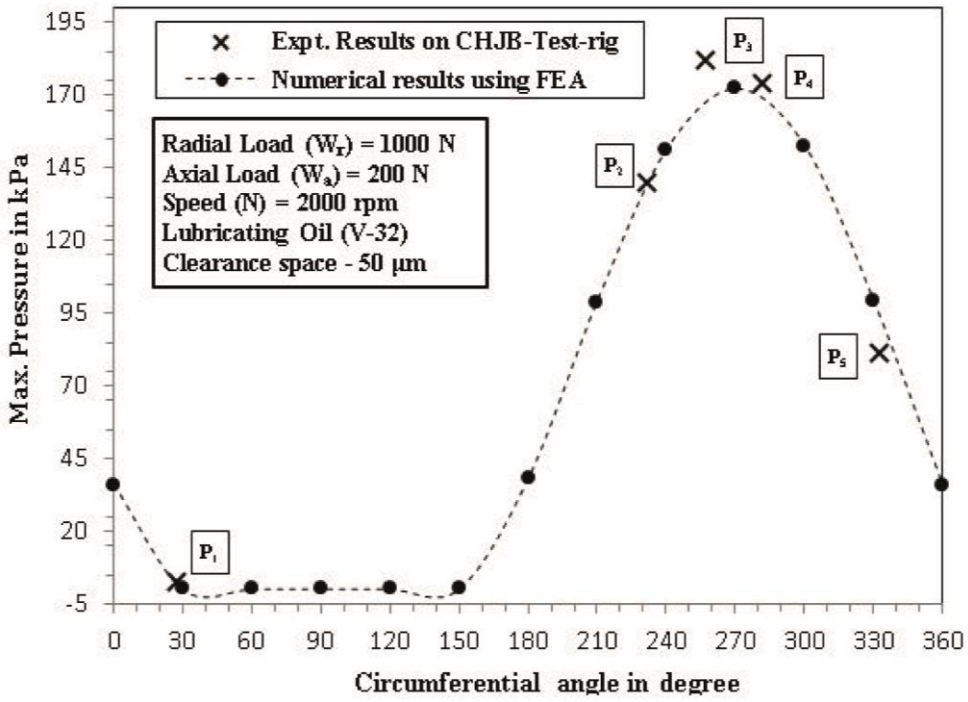

Figure 7: Validation of FEA results with experimental results on customized CHJB-test-rig.

4.1 Radial and axial load carrying capacity ($\bar{W}_r, \bar{W}_a$)

Geometrical parameters alter the pressure distribution in the clearance space and load carrying capacity of the bearing. In this section, Radial and axial load carrying capacity are presented as a function of eccentricity ratio for the conical bearing. Radial load capacity ($\bar{W}_r$) in conical hydrodynamic journal bearing is increases with the increase of aspect ratio. Figure 8 shows the effect of aspect ratio (λ = 0.5, 0.8, 1.0) on conical hydrodynamic journal bearing of semi cone angle (γ = 10°) and it is found that value of $\bar{W}_r$ is increased in the order of 6.3 times for bearing of aspect ratio (λ = 1) as compared to bearing of aspect ratio (λ = 0.5), when bearing operating at an eccentricity ratio (ε = 0.5) and journal speed 5.2 m/s. Figure 9 shows the influence of aspect ratio (λ = 0.5, 0.8, 1.0) on the axial load carrying capacity ($\bar{W}_a$) of the conical hydrodynamic journal bearing of semi cone angle (γ = 10°) and it is found that the increase in the value of $\bar{W}_a$ is in the order of 4.47 times for bearing of aspect ratio (λ = 1) as compared to the bearing of aspect ratio (λ = 0.5) when bearing is operating at an ecc. ratio (ε = 0.5) and journal speed 5.2 m/s.

4.2 Direct stiffness coefficient ($\bar{S}_{11}, \bar{S}_{22}$)

The variations of the direct stiffness coefficient $\bar{S}_{11}$ in *X*-direction and $\bar{S}_{22}$ in *Z*-direction have been illustrated in Fig. 10 and Fig. 11 respectively for aspect ratio (λ = 0.5, 0.8, 1.0) and semi cone angles (γ = 10°).The values of fluid film stiffness coefficients are anticipated to change with an increase in the value of aspect ratio (λ) as the quantity of lubricant is increased in clearance space. This is also due to the distribution of pressure and fluid film reaction with a change in aspect ratio. It is found that for the conical bearing of semi cone angle (γ = 10°), stiffness coefficients $\bar{S}_{11}$ and

$\bar{S}_{22}$ increases in the order of 5.14 and 5.96 times respectively for bearing with an aspect ratio (λ = 1) as compared to the bearing of aspect ratio (λ = 0.5), when bearing operated at an eccentricity ratio (ε = 0.5) and journal speed 5.2 m/s and shown in Fig. 10 and Fig. 11 respectively. The values of cross coupled stiffness coefficients ($\bar{S}_{12}$ and $\bar{S}_{21}$) is also calculated in the present work but for the sake of brevity, the plots of cross coupled stiffness coefficients have not been shown in this paper.

4.3 Direct damping coefficient ($\bar{C}_{11}$, $\bar{C}_{22}$)

In fluid film bearing, direct damping coefficients enhance the performance by damping out the oscillations with an increase in the value of aspect ratio and semi-cone angle. In the present work the variations of the direct damping coefficient ($\bar{C}_{11}, \bar{C}_{22}$) has been discussed for various aspect ratio and semi cone angle (γ = 10°) as shown in Fig. 12 and Fig. 13 respectively. It is found that damping coefficients $\bar{C}_{11}$ and $\bar{C}_{22}$ increases in the order of 4.46 and 5.63 times respectively for bearing of aspect ratio (λ = 1) as compared to bearing of aspect ratio (λ = 0.5), when bearing of semi cone angle (γ = 10°) is operated at an eccentricity ratio (ε = 0.5) and journal speed 5.2 m/s. Due to less resistance of fluid film in compact journal bearing (λ = 0.5), the value of $\bar{C}_{11}$ is reduced and quite significant for bearing at higher eccentricity ratio (ε = 0.6) as shown in Fig. 12. It is also observed that damping coefficient ($\bar{C}_{11}, \bar{C}_{22}$) increase significantly at higher eccentricity ratio (ε = 0.6), when the bearing size increases in terms of aspect ratio from 0.5 to 1.0. It is also observed that at low eccentricity ratio conical journal bearing of aspect ratio (λ = 0.5) performs better from the stability point of view for damping out oscillations. In this work damping coefficient parameters are studied for static load conditions for particular eccentricity ratio, hence the change in position of journal center with respect to bearing center is assumed to be negligible and this might be the reason for journal speed (v) is not influencing the damping parameter. In this work for sake of brevity; results of cross-coupled damping coefficients have not been presented in this paper.

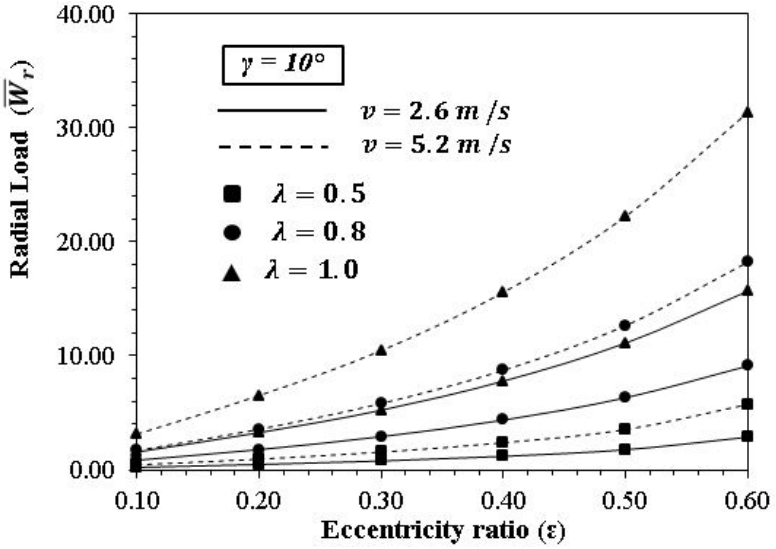

Fig.ure 8: Variation in radial load ($\bar{W}_r$) w.r.t. eccentricity ratio (ε) for speed (v = 2.6, 5.2 m/s).

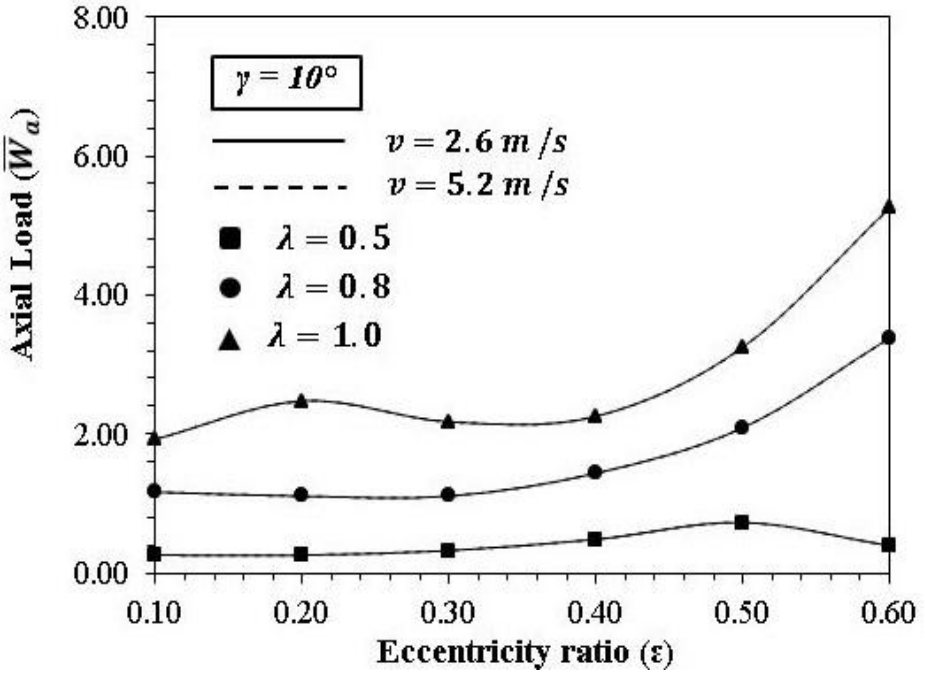

Figure 9: Variation in axial load ($\bar{W}_a$) w.r.t. eccentricity ratio (ε) for speed (v = 2.6, 5.2 m/s).

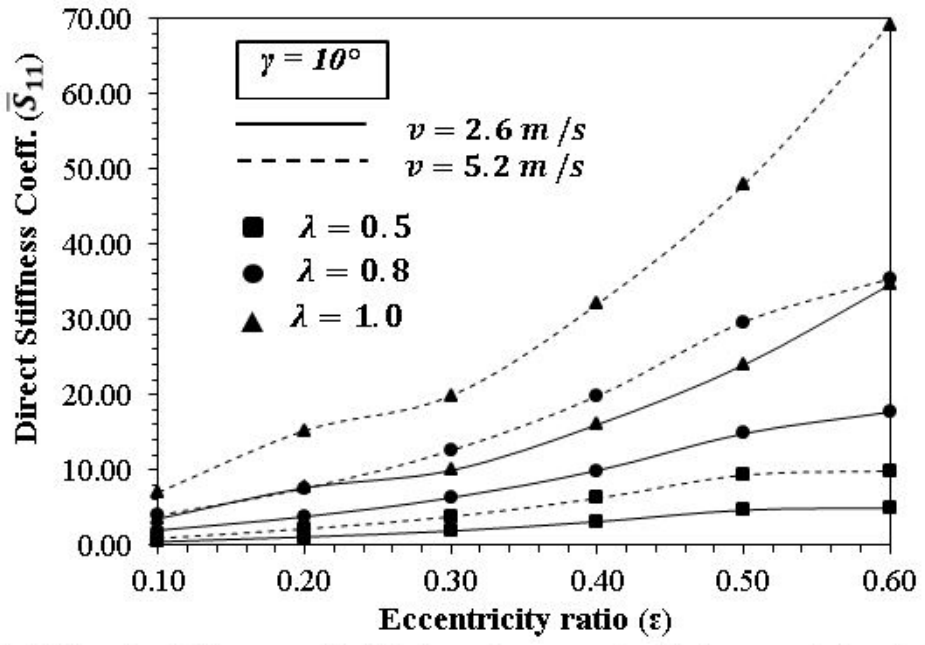

Figure 10: Variation in stiffness coeff.($\bar{S}_{11}$) w.r.t. ecc. ratio (ε) for speed (v = 2.6, 5.2 m/s).

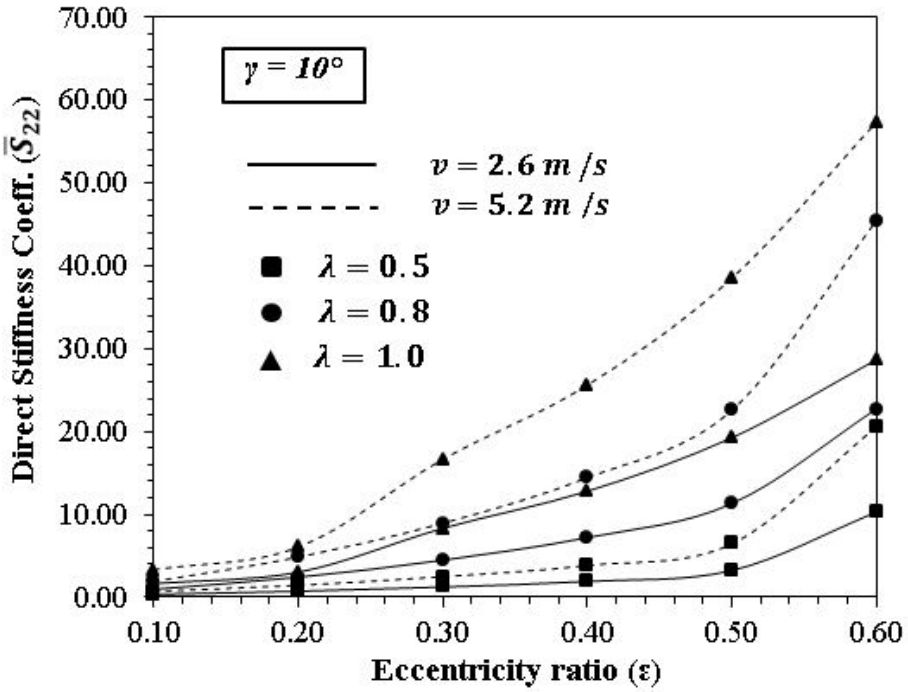

Figure 11: Variation in stiffness coeff. ($\bar{S}_{22}$) w.r.t. ecc. ratio (ε) for speed (v = 2.6, 5.2 m/s).

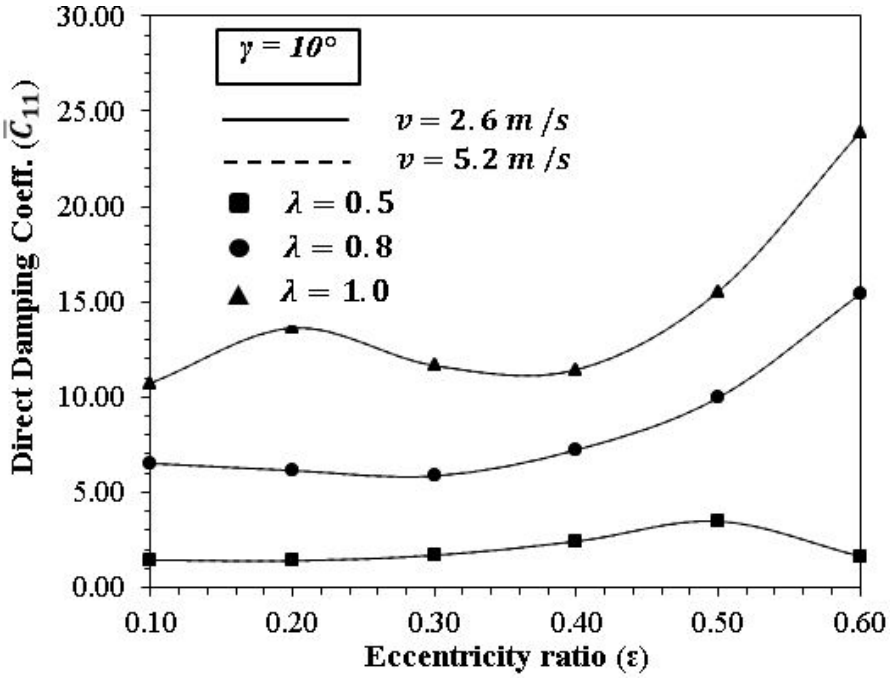

Figure 12: Variation in damping coeff. ($\bar{C}_{11}$) w.r.t. ecc. ratio (ε) for speed (v = 2.6, 5.2 m/s).

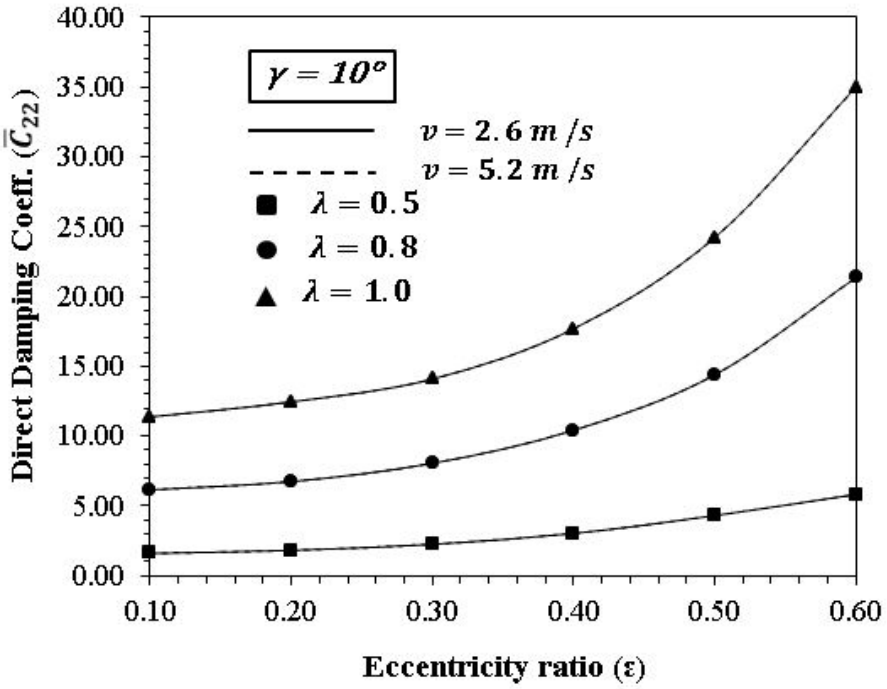

Figure 13: Variation in damping coeff. ($\bar{C}_{22}$) w.r.t. ecc. ratio (ε) for speed (v = 2.6, 5.2 m/s),

4.4 Stability threshold speed margin ($\bar{\omega}_{th}$)

In the present paper, linear stability analysis has been carried out by using a perturbation method around the steady-state equilibrium motion of journal in clearance space. The influence of aspect ratio (λ = 0.5, 0.8, 1.0) on non-dimensional threshold speed ($\bar{\omega}_{th}$) of bearing for semi cone angle 10° and variation in eccentricity ratio (ε) up to 0.6 is shown in Fig. 14. In this study, it is observed that with a decrease in aspect ratio from 1.0 to 0.5, the value of $\bar{\omega}_{th}$ is slightly increased for the bearing of semi-cone angle 10°. In order to get better performance, considering the stability of bearing in terms of threshold speed($\bar{\omega}_{th}$), a judicious selection of aspect ratio or bearing size is essential. Therefore, it is anticipated from this study that the influence of aspect ratio on performance parameters for various conical hydrodynamic journal bearing is significant and these should be incorporated at bearing design stage. It was found that non-dimensional threshold speed decreases with the increase of aspect ratio. Hence the size of the conical hydrodynamic journal bearing in terms of aspect ratio is important for stability performance in terms of threshold speed. It is also observed that when the aspect ratio of hydrodynamic conical journal bearing is considered less than unity (λ = 0.5), threshold speed decreases up to a certain value of eccentricity ratio (ε = 0.3) and then starts to increasing rapidly at higher eccentricity ratio (ε = 0.5). It was found that $\bar{\omega}_{\text{th}}$ is decreasing with increase in journal relative velocity (v), whereas threshold speed (Ω) is having almost constant value for any set of system. Hence, here conferred that threshold speed (Ω) for conical hydrodynamic journal bearing is also safe for high speed at 5.2 m/s.

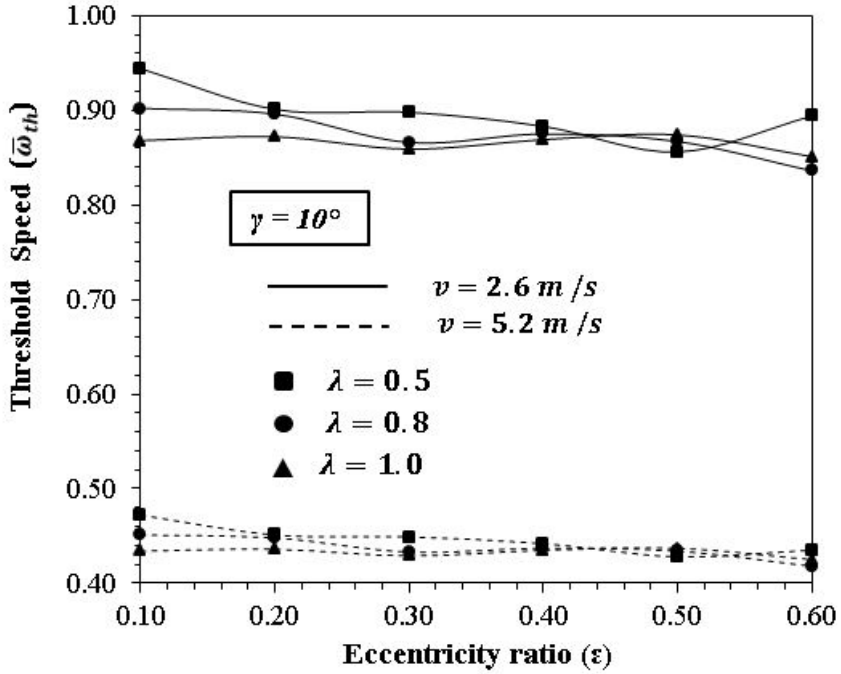

Figure 14: Variation in threshold speed ($\bar{\omega}_{th}$) w. r. t. ecc.ratio (ε), operating speed (v = 2.6, 5.2 m/s).

5.0 CONCLUSIONS

In this study, stability behaviour of short length conical hydrodynamic journal bearing is presented for semi-cone angle (γ = 10°), aspect ratio (λ = 0.5, 0.8, 1.0) and journal operating speeds (v = 2.6, 5.2 *m/s*) for variation in eccentricity ratio (ε) up to 0.6. Based on these results, the following conclusions are summarized here:

(a) Radial load ($\bar{W}_r$) and axial load ($\bar{W}_a$) carrying capacity of bearing increases with the increase of aspect ratio and an increase of journal relative velocity with respect to the rigid conical bearing.

(b) The value of stiffness coefficient ($\bar{S}_{11}$, $\bar{S}_{22}$) increases with increase in value of aspect ratio from λ = 0.5 to λ = 1. Relative velocity of the journal also influences the stiffness parameter at higher eccentricity ratio.

(c) Damping coefficients ($\bar{C}_{11}$, $\bar{C}_{22}$) enhanced the performance of bearing with an increase of aspect ratio by damping out the oscillations. The value of $\bar{C}_{11}$, $\bar{C}_{22}$ increases significantly at higher eccentricity ratio (ε = 0.6), when the aspect ratio increases from 0.5 to 1.0.

(d) The effect of aspect ratio and journal rotational speed is more pronounced on threshold speed ($\bar{\omega}_{th}$) and it is found that the value of $\bar{\omega}_{th}$ marginally decreases in all the configuration of bearing with an increase of eccentricity ratio. Small size bearing of aspect ratio λ = 0.5 performs better in terms of threshold speed ($\bar{\omega}_{th}$) in the lower range of eccentricity ratio up to 0.3. It is also observed that for the conical bearing of 10° and eccentricity ratio up to 0.6 the journal threshold speeds ($\bar{\omega}_{th}$) is more unstable for the small size of bearing.

ACKNOWLEDGEMENT

The financial support from the All India Council for Technical Education (AICTE), New Delhi-India under Research Promotion Scheme (RPS) Ref. No. 8-221/RIFD/RPS/Policy-1/2014-15 is gratefully acknowledged. The author is grateful to the Director, Veermata Jijabai Technological Institute (V.J.T.I), Mumbai and Principal, K. J. Somaiya College of Engineering (KJSCE), Mumbai for all support provided for this study is respectfully acknowledged.

REFERENCES

Bassani, R., & Piccigallo, B. (1992). Hydrostatic lubrication. Elsevier Science Publishers B.V, Amsterdam.

Bhattacharya, A., Dutt, J. K., & Pandey, R. K. (2017). Influence of hydrodynamic journal bearings with multiple slip zones on rotor-dynamic behavior. Journal of Tribology, 139, 061701-1-11.

Chen, G., Yang, Y., Ma, R., & Chen, B. (2015). Modeling cone self-acting gas lubrication bearing dynamics. Procedia Engineering, 126, 416-420.

Czaban, A. (2013). CFD analysis of pressure distribution in slide conical bearing lubricated with non-newtonian oil. Journal of KONES Powertrain and Trans., 20, 117-124

Ettles, C., & Svoboda, O. (1975). The Application of Double Conical Journal Bearings in High Speed Centrifugal Pumps—Parts 1 and 2. Proceedings of the Institution of Mechanical Engineers, 189(1), 221-230.

Gamal, A. R. M. (2004). The fluid flow in the thin films between the immobile conic surfaces. Applied Mathematics and Computation, 153, 59–67.

Gamal, M. A. R., & Al-Hanaya, A. M. (2014). The MHD flow of a non-newtonian power law through a conical bearing in a porous medium. Journal of Modern Physics, 5, 61-67.

Garg, H. C. (2015). Stability analysis of slot-entry hybrid journal bearings operating with non-newtonian lubricant. Jurnal Tribologi, 6, 1-23.

Hong, G., Xinmin, L., & Shaoqi, C. (2009). Theoretical and experimental study on dynamic coefficients and stability for a hydrostatic/ hydrodynamic conical bearing. Transactions of the ASME: Journal of Tribology, 131, 041701-1-7.

Javorova, J., Sovilj, B., Andonov, I., & Sovilj-Nikic, I. (2009). Stability and imbalance response of a rigid rotor supported on plain journal bearing. Proceedings of the 7th Conference on Tribology, Tribology Journal Bultrib, Temto Pub., Sofia, 176-184.

Khakse, P. G., Phalle, V. M., & Mantha, S. S. (2016). Performance analysis of a nonrecessed hybrid conical journal bearing compensated with capillary restrictors. Journal of Tribology, 138(1), 011703.

Kim, H., Jang, G., & Ha, H. (2012). A generalized Reynolds equation and its perturbation equations for fluid dynamic bearings with curved surfaces. Tribology International, 50, 6-15.

Kim, K., Lee, M., Lee, S., & Jang, G. (2017). Optimal design and experimental verification of fluid dynamic bearings with high load capacity applied to an integrated motor propulsor in unmanned underwater vehicles. Tribology International, 114, 221–233.

Korneev, A. Y. (2012). Influence of turbulence on the static characteristics of conical journal bearings. Russian Engineering Research, 32, 338-342.

Korneev, A. Y., & Yaroslavtsev, M. M. (2010). Dynamic characteristics of conical multiple-pad hydrodynamic liquid-friction bearings. Russian Engineering Research, 30, 365-369.

Lund, J. W. (1974). Stability and damped critical speeds of a flexible rotor in fluid-film bearings. Journal of Engineering for Industry, 96(2), 509-517.

Murthy T. S. R. (1981). Analysis of multi-scallop self-adjusting conical hydrodynamic bearings for high precision spindles. Tribology International, 14, 147-150.

Rahmani, F., Dutt, J. K., & Pandey R. K. (2016a). Performance behavior of elliptical-bore journal bearings lubricated with solid granular particulates. Particuology, 27, 51 – 60.

Rahmani, F., Dutt, J. K., & Pandey R. K. (2016b). Dynamic characteristics of finite width journal bearing lubricated with powders. Procedia Engineering, 144, 841-848.

Rajput, A. K., & Sharma, S. C. (2013). Analysis of externally pressurized multirecess conical hybrid journal bearing system using micropolar lubricant. Proceedings of the Institution of Mechanical Engineers, Part J: Journal of Engineering Tribology, 227(9), 943-961.

Ram, N. (2016a). Performance of non-recessed hole-entry hybrid journal bearing operating under turbulent regime. Jurnal Tribologi, 8, 12-26.

Ram, S. (2016). Numerical analysis of capillary compensated micropolar fluid lubricated hole-entry journal bearings. Jurnal Tribologi, 9, 18-44.

Rana, N. K., Gautam, S. S., Verma, S. & Rahmani, F. (2016). On the stiffness and damping coefficients of the constant flow valve compensated conical hydrostatic journal bearing with micropolar lubricant. Procedia Technology, 23, 42-50.

San Andres, L. A. (1991). Effect of Eccentricity on the Force Response of a Hybrid Bearing. Tribology transactions, 34(4), 537-544.

Sharma, S. C., Phalle, V. M., & Jain, S.C. (2011a). Performance analysis of a multirecess capillary compensated conical hydrostatic journal bearing. Tribology International, 44(5), 617-626.

Sharma, S. C., Phalle, V. M., & Jain, S.C. (2011b). Influence of wear on the performance of a multirecess conical hybrid journal bearing compensated with orifice restrictor. Tribology International, 44(12), 1754-1764.

Sharma, S., & Awasthi, R. K. (2016). Effect of aspect ratio on the performance and stability of hydrodynamic journal bearing. International Journal of Advanced Research and Innovation, 4, 96-105.

Sharma, S., & Awasthi, R. K. (2017). Effect of aspect ratio on the performance of hydrodynamic journal bearing operating under wear. International Journal of Theoretical and Applied Mechanics, 12, 497-522.

Sharma, S., & Krishna, C. M. (2015). Effect of L/D ratio on the performance of two-lobe pressure dam bearing: micropolar lubricated. Advances in Tribology, 2015, 182713-1-7.

Yadav, S. K., & Ram, N. (2018). Transient response of two lobe aerodynamic journal bearing. Jurnal Tribologi, 16, 1-14.

Yousif, A. E., & Nancy, S. M. (1994). The lubrication of conical journal bearings with bi-phase (liquid-solid) lubricants. Wear, 172, 23-28.